A Parameterized Geometric Magnetic Field Calibration Method for Vehicles with Moving Masses with Applications to Underwater Gliders

Brian Claus and Ralf Bachmayer

Abstract The accuracy of magnetic measurements performed by autonomous vehicles is often limited by the presence of moving ferrous masses. This work proposes a third order parameterized ellipsoid calibration method for magnetic measurements in the sensor frame. In this manner the ellipsoidal calibration coefficients are dependent on the locations of the moving masses. The parameterized calibration method is evaluated through field trials with an autonomous underwater glider equipped with a low power precision fluxgate sensor. These field trials were performed in the East Arm of Bonne Bay, Newfoundland in December of 2013. During these trials a series of calibration profiles with the mass shifting and ballast mechanisms at different locations were performed before and after the survey portion of the trials. The nominal ellipsoidal coefficients were extracted using the full set of measurements from a set of calibration profiles and used as the initial conditions for the third order polynomials. These polynomials were then optimized using a gradient descent solver resulting in a RMS error between the calibration measurements and the local total field of 28 nT and 17 nT for the first and second set of calibration runs. When the parameterized coefficients are used to correct the magnetic measurements from the survey portion of the field trials the RMS error between the survey measurements and the local total field was 124 nT and 69 nT when using the first and second set of coefficients.

1 Introduction

The use of underwater vehicles as a platform for oceanic research is an excellent way to collect high quality data in a challenging environment. Long range AUVs,

Brian Claus
Memorial University of Newfoundland, Faculty of Engineering e-mail: bclaus@mun.ca

Ralf Bachmayer
Memorial University of Newfoundland, Faculty of Engineering e-mail: bachmayer@mun.ca

capable of travelling thousands of kilometers before needing to be recovered are recently the focus of significant interest [10], [9]. Underwater gliders are a type of long range underwater vehicle, however, they require surface access for navigation, have limited speed and require vertical translation for forward movement [14]. For these vehicles minimizing energy consumption is one of the primary design and operational goals.

The use of magnetic field measurements as a heading reference for navigation in underwater vehicles has been well established [7]. In recent work earth magnetic information has also been suggested for possible use in total-field map based relative navigation techniques [6, 16]. This use of magnetic measurements for online navigational aiding is the motivation for this research. In such a system, magnetic measurements are capable of augmenting a terrain relative navigation scheme in regions of low terrain variability or when the terrain is beyond the range of the vehicle's acoustic sensors. However, an online implementation of a magnetic aided navigation system has not been realized. This lack of progress has been limited by the challenges involved in instrumenting and calibrating an underwater vehicle for accurate online magnetic measurements and the lack of suitably high resolution magnetic maps.

Scalar calibration of vector magnetometers has shown to be a robust method of calibration based on a geometric fit to an ellipsoid [17, 2, 13]. Another method relies on projecting the measurement vector onto the horizontal plane and fitting an ellipse [5, 8]. Of these methods, the second is more suited to vehicles which have limitations in the controllable degrees of freedom such as an underwater glider. However, it requires a precision attitude reference to rotate the magnetic measurements to the horizontal plane which is infeasible on an underwater glider due to their relatively large energy consumption. Additionally, long range underwater vehicles, and underwater gliders in particular, require additional effort to calibrate the magnetic field measurements. This extra effort is due to the use of an adjustable internal mass for attitude control which is typically composed of a battery pack and therefore includes hard and soft magnetic materials.

As a step towards a real time total field magnetically aided navigation system this work examines suitable methods for calibrating, instrumenting and performing magnetic measurements with an underwater glider. The variable locations of the mass shifting and ballast mechanisms on the underwater glider provide an additional challenge for calibrating the magnetic measurement system. As such, a parameterized calibration method is presented which fits polynomial functions to the calibration parameters based on the actuator locations. To this end the theory for a nominal geometric calibration and a parameterized geometric calibration method is presented and the underwater glider equipped with the magnetic instrumentation developed for this work is introduced. Lastly, the calibration procedures are demonstrated on field data gathered using the underwater glider during trials in the East Arm of Bonne Bay. The calibrated data are compared with magnetic anomaly models produced from prior aeromagnetic surveys of the region.

2 Calibration Methods

Measurements of the earth's magnetic field must be calibrated in order to remove the effects of the sensing platform. These effects can be due to instrument non-linearities as well as hard and soft magnetic effects.

2.1 Nominal Geometric Calibration

If the moving masses in the vehicle are held stationary the hard and soft magnetic effects from the vehicle as well as scaling, bias and other instrument errors may be calibrated for using geometric batch methods [17, 2, 13]. These methods assume a constant magnetic field and rely on rotations of the instrument through the calibration space such that an ellipsoid may be fit to the data.

An ideal magnetic sensor at a fixed location produces measurements with a constant magnitude resulting in the data lying on the surface of a sphere, centered on the origin with the radius equal to this magnitude. Distortions due to the sensor errors and the vehicle hard and soft magnetic effects have been shown to cause the measurements to be translated, rotated and scaled such that the sphere becomes an ellipsoid. The problem of finding this set of translation, rotation and scaling coefficients can be expressed in matrix notation as

$$[\mathbf{M},\mathbf{S},\mathbf{T}] = G(\mathbf{H}_r) \tag{1}$$

where $\mathbf{M}$, $\mathbf{S}$, and $\mathbf{T}$ are the rotation, scaling and translation matrices that are representative of the ellipsoidal fit $G()$ to the raw magnetic data vector $\mathbf{H}_r$. Geometrically, the translation coefficients are the distance from the center of the ellipsoid to the origin, the scaling coefficients are the magnitudes of the major and minor ellipsoid axes and the rotation coefficients are the rotations of the major and minor axes of the ellipsoid. The ellipsoid equation representing the relationship between the raw magnetic data and the corrected data is written as

$$\mathbf{H}_r = H_e^{-1}\mathbf{S}\mathbf{M}\mathbf{H}_c + \mathbf{T} \tag{2}$$

The raw magnetic data may then be translated, rotated and scaled accordingly by re-arranging the ellipsoid equation to

$$\mathbf{H}_c = H_e\mathbf{S}^{-1}\mathbf{M}^{-1}(\mathbf{H}_r - \mathbf{T}) \tag{3}$$

where $\mathbf{H}_c$ is the calibrated magnetic data vector in the sensor frame. This calibration procedure normalizes the magnitude of the magnetic measurements due to the product of the inverse of the scaling coefficients. To give the calibrated values units, the normalized values must be scaled by the magnitude of the local magnetic field at the calibration location H_e which often may be approximated from the International Geomagnetic Reference Field (IGRF) [4]. The IGRF does not include many of the higher frequency components and the local magnetic anomalies. If a local anomaly map is available these anomaly values may be included as in

$$H_e = ||\mathbf{H}_{IGRF}|| + H_a \tag{4}$$

where H_a is the magnitude of the magnetic anomalies at the calibration locations. The resulting values given by $\mathbf{H}_c$ are the calibrated measurements of the magnetic field for a vehicle with fixed locations of the hard and soft magnetic influences and no significant electrical currents.

2.2 Parameterized Geometric Calibration

For vehicles with moving hard or soft magnetic parts that have a number of steady state values a parameterized version of the geometric calibration method is proposed. In this method the nominal geometric calibration procedure from section 2.1 is performed on data gathered from a number of different steady state values for each of the moving parts. The fixed calibration parameters are used as the initial conditions for an iterative gradient decent solver which optimizes a third order function with each of the moving masses as parameters. In the case of underwater gliders, the primary parameters are the moving mass mechanism used for fine control of the vehicle pitch and the ballast mechanism which is responsible for the large pitch and buoyancy changes between diving and climbing. The geometric fitting then becomes of the form

$$[\mathbf{M}, \mathbf{S}, \mathbf{T}](p_m, p_b) = G(\mathbf{H}_r(p_m, p_b)) \tag{5}$$

where each of the rotation, translation and scaling coefficients is a function of the moving mass location p_m and the ballast piston location p_b. The parameterized functions are found by fitting polynomials to the set of individual calibration coefficients found for a geometric fit to the magnetic measurements for a given moving mass and ballast location. The parameterized ellipsoid equation is similarly given as

$$\mathbf{H}_r = H_e^{-1}\mathbf{S}(p_m, p_b)\mathbf{M}(p_m, p_b)\mathbf{H}_c + \mathbf{T}(p_m, p_b) \tag{6}$$

Upon re-arranging, the raw magnetic data may be corrected by computing the translation, rotation and scaling matrices for a given moving mass and ballast location as in

$$\mathbf{H}_c = H_e\mathbf{S}(p_m, p_b)^{-1}\mathbf{M}(p_m, p_b)^{-1}(\mathbf{H}_r - \mathbf{T}(p_m, p_b)) \tag{7}$$

The polynomial functions in this case are of third order and take the form of

$$\begin{aligned} c_0 p_m^3 + c_1 p_b^3 + c_2 p_m^2 + c_3 p_b^2 + c_4 p_m^2 p_b + c_5 p_m p_b^2 \\ + c_6 p_m p_b + c_7 p_m + c_8 p_b + c_9 \end{aligned} \tag{8}$$

resulting in a total of 90 coefficients required for a two parameter calibration problem.

3 Instrumentation

An underwater glider's energy is provided by onboard batteries which gives it an endurance of around one month when using alkaline primary cells and six months when using lithium primary cells. In a standard configuration of a vehicle equipped only with a conductivity, temperature and pressure sensor (CTD), the vehicle uses an average power of around one Watt. To not significantly impact the endurance or range of the vehicle, additional sensors should use as little power as possible. Therefore, to instrument an underwater glider with a precision magnetic sensor, the power consumption of the device must remain low to minimize the impact on the vehicle's endurance.

While progress is being made towards lower power cesium vapour magnetometers which would be well suited to integration in mobile platforms, the power consumption of presently available devices still remains on the order of Watts [15, 12]. Fluxgate sensors, on the other hand, have power requirements down to the level of 10s of milliwatts. For this reason the chosen sensor is a low power tri-axial Mag-648 fluxgate magnetometer by Bartington Instruments which consumes around 14 milliwatts [1]. Low power fluxgates of this type are often subject to higher degrees of noise, orthogonality errors, and offset errors than higher power versions [11]. While the impact of the higher noise is mitigated through low frequency sampling requirements, the orthogonality errors and offset errors require careful calibration. Additionally, the offset error settles to a slightly different value each time the sensor is powered on requiring the sensor to remain energized once calibrated.

The fluxgate sensor is mounted in a strap-down configuration in the vehicle's payload bay. The device is powered by a set of independent batteries and is sampled using an isolated 24-bit sigma-delta analog to digital converter (ADC). This ADC uses several different internal low pass filters and modifies the filter coefficients based on the sampling rate selected. The effective resolution of the device is therefore variable with the sampling rate. The inputs to the ADC have anti-aliasing filters with a corner frequency of 0.33 Hz to mitigate high frequency noise from the electronics and other systems. The ADC uses the serial peripheral interface (SPI) to send the data to the glider payload computer where it is logged at a frequency of 0.25 Hz. The ADC used has a single digitizer and samples of each channel are taken at different times requiring the time stamp of each channel's measurement to be recorded such that the measurements may be interpolated to the same time base. The electrical current drawn by the fluxgate and its electronics is around 4.5 mA. As a result of this low energy consumption, a single set of three AA alkaline cells connected in series will power the fluxgate and its electronics for one month. The goal of not influencing the endurance of the underwater glider while staying within the size and weight requirements for the payload are therefore achieved.

4 Field Trials

Field trials using the magnetic fluxgate sensor installed on a 200 meter Slocum Electric glider were performed to evaluate the efficacy of making magnetic measurements using this platform. The parameterized calibration field trials took place in December, 2013 in the East Arm of Bonne Bay, Newfoundland. In these trials the underwater glider was launched from the small aluminum boat Freezy as illustrated in Fig. 1 and after launch was controlled from the Bonne Bay Marine Station. During the deployment there were light winds and the air temperature was around

Fig. 1 The Bonne Bay Marine Station's boat Freezy shown with the Slocum autonomous underwater glider during the parameterized trials in December 2013.

-10 degrees Celsius. Recovery of the vehicle was originally planned for December 12th but had to be delayed due to strong winds. The vehicle was left to loiter in the lee of the head on Norris Point until a lull in the winds on the 13th allowed the recovery of the vehicle.

After the deployment, a series of clockwise calibration spirals were performed with the vehicle commanded to set the movable battery once during each ascent or descent to achieve a certain pitch according to a look up table. In this way five different battery locations were tested for two different ballast conditions. The ballast was also set to a single value, once for each ascent or descent. Each calibration run therefore consisted of a single spiralling descent and ascent with the ballast and battery at a fixed location and took around 30 minutes to complete. Another full calibration procedure was repeated prior to recovery. The calibration runs are summarized in Table 1.

Table 1 Calibration runs for the parameterized magnetic calibration trials

Run	Direction	p_b $[cm^3]$	Pitch [deg]	p_m Trial 1 [in]	p_m Trial 2 [in]
1	Dive	-200	-14	0.272	0.226
2	Climb	200	14	-0.181	-0.139
3	Dive	-200	-18	0.380	0.274
4	Climb	200	18	-0.234	-0.191
5	Dive	-200	-22	0.428	0.375
6	Climb	200	22	-0.289	-0.246
7	Dive	-200	-26	0.491	0.400
8	Climb	200	26	-0.344	-0.300
9	Dive	-200	-30	0.527	0.472
10	Climb	200	30	-0.401	-0.348

The vehicle was then flown in a criss-cross pattern down into the bay and back again with a commanded pitch of plus or minus 26 degrees and a commanded ballast of plus or minus 200 cm^3. The calibration locations along with the vehicle track-line are shown against the local residual magnetic field in Fig. 2.

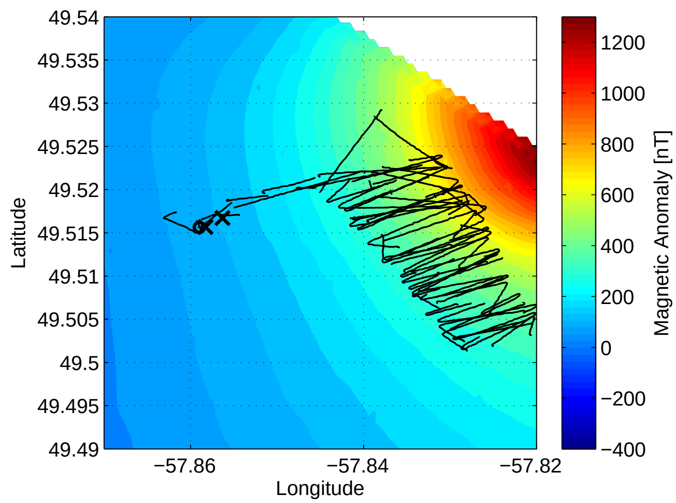

Fig. 2 Calibration locations (x's) and the Bonne Bay Trials track-line (black line) starting from the circle and proceeding to crisscross south and then north in the East Arm of Bonne Bay. The residual magnetic grid of the Bonne Bay region is shown in the background.

To provide reference measurements, aeromagnetic data overlapping the East Arm of Bonne Bay was used from the Newfoundland and Labrador Geoscience Atlas [3]. Unfortunately, the East Arm is split in half by the boundary of two different surveys, the 2009 Corner Brook survey and the 2012 Offshore Western Newfoundland survey. To obtain a reference grid both residual magnetic grids were upward continued

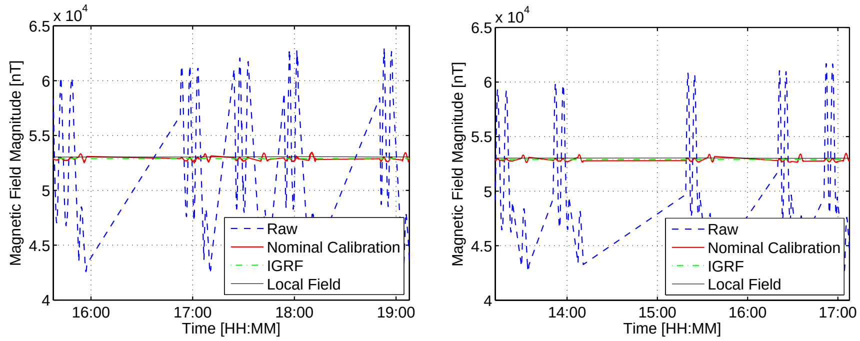

Fig. 3 Magnitude of the magnetic data using the nominal calibration method before and after correction shown against the IGRF values for the Bonne Bay field trials using the first (left) and second (right) set of calibration coefficients

to a constant altitude of 90 meters. The grids were then combined, using the average value in the regions of overlap. A mask was applied to these larger grids to limit the region to the area of the East Arm of Bonne Bay. To smooth any discontinuities, 20 passes of a 3x3 Convolution (Hanning) filter were applied to remove the high frequency content introduced by combining the grids. The resulting grid is shown in Fig. 2.

For the parameterized calibration method, an initial global fit of the nominal geometric method was performed by using the full set of raw measurements from each of the calibration runs. To constrain the ellipsoid in this initial fit it was necessary to make the x and z scaling values equal as there were no calibration measurements in the "northern hemisphere" of the calibration space. Additionally, the ellipsoid was constrained in rotation such that $\mathbf{M} = \mathbf{I}$. The global fit was then used as the initial conditions for the parameterized equations by setting the c_9 coefficients from Eqn. 8 to be equal to the ellipsoid's scaling, translation and rotation coefficients. The parameterized equations were then adjusted using a gradient descent optimization scheme by minimizing the error between the local total field and measured values. In this optimization scheme the local total field was computed from the IGRF model and the magnetic anomaly value at the calibration locations. The resulting magnitude of the calibrated measurements are shown in Fig. 3.

The nominal geometric method results in a root mean square error between the total field estimate from the IGRF and aeromagnetic data and the calibrated data of 153 nT and 145 nT for the first and second set of calibration runs. The resulting magnitude of the calibration measurements, corrected with the parameterized coefficients are shown in Fig. 4.

The parameterized geometric method results in a root mean square error between the total field estimate from the IGRF and aeromagnetic data and the calibrated data of 29 nT and 17 nT for the first and second calibration trials. Each of these sets of parameters is then used to correct the magnetic data gathered during the remainder of the deployment as shown in Fig. 5. In correcting this data the calibration coeffi-

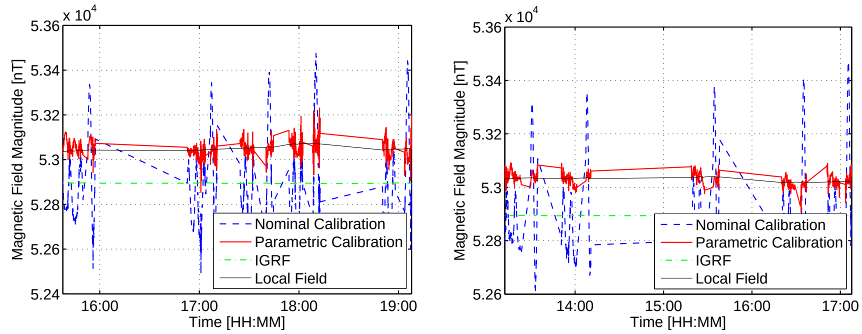

Fig. 4 Magnitude of the magnetic data using the nominal and parameterized calibration method with the data from the first (left) and second (right) set of trials shown against the IGRF and local field values for the Bonne Bay trials

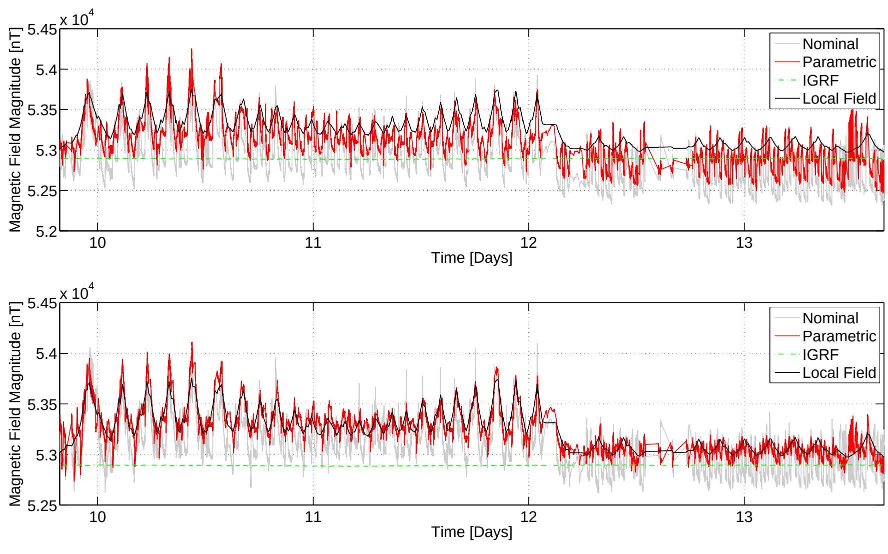

Fig. 5 Magnetic data collected during the Bonne Bay deployment in December 2013 shown against the IGRF and local field values calibrated using the first (top) and second (bottom) set of nominal and parameterized calibration coefficients

cients are assumed to be constant. As such the mean of the local magnetic field at the calibration locations, H_e, is used for each set of calibration coefficients.

The calibrated magnetic measurements gathered by the glider may then be compared to the residual magnetic grids. The resulting interpolated values have a constant bias when compared to the complete set of glider magnetic measurements. Additionally, the glider data contains significantly more high frequency components than the aeromagnetic grids. These differences are attributed to the aeromagnetic

Table 2 The RMS errors between the magnetic anomaly map values and the calibrated measurements using the first and second set of nominal and parametric calibration coefficients during the Bonne Bay field trials.

	Nominal	Parametric
Trial 1	207 nT	124 nT
Trial 2	136 nT	69 nT

data being collected at a higher altitude reducing the high frequency signatures present in the reference data as well as the significant low-pass filtering applied during the gridding operations.

The first set of parameterized calibration coefficients perform well only for a short period of time. After the first day or so of measurements, there is a significant change in bias present in the measured values when compared to the local field. The second set of parameterized calibration coefficients does not display this change in bias, remaining consistently around the level of the local field. This difference is thought to be due to the temperature dependence of the sensor. The first calibration run was performed immediately after launch while the vehicle had been at a temperature of less than -10^o Celsius. The second calibration run was performed after the data collection before retrieval allowing the sensor adequate time to warm up to the water temperatures of around 2^o Celsius. The measurements calibrated using the second set of parameterized coefficients were deemed more accurate for this reason and are shown next to the residual magnetic field values from the vehicle locations in Fig. 6.

The measured magnetic anomaly data calibrated using the second set of parameterized calibration coefficients is in reasonable agreement with the residual magnetic field data from the aeromagnetic surveys with RMS errors indicated in Table 2. Additionally, the parameterized geometric calibration method improves significantly upon the nominal geometric calibration method. This agreement indicates that the parameterized calibration method is effective for calibration of magnetic measurements performed from a vehicle with moving masses. The drawback of this method are the increased number of calibration runs that need to be performed over the nominal calibration method. However, while the parameterized calibration method takes longer to perform, it constrains the calibration space to a higher degree than the nominal method for the limited maneuvering space available to the underwater glider resulting in a better calibration.

5 Conclusions

Augmenting underwater relative navigation methods with total field magnetic measurements and a-priori magnetic anomaly grids has been proposed previously in several theoretical studies. Evaluating this proposition in practice is challenging due

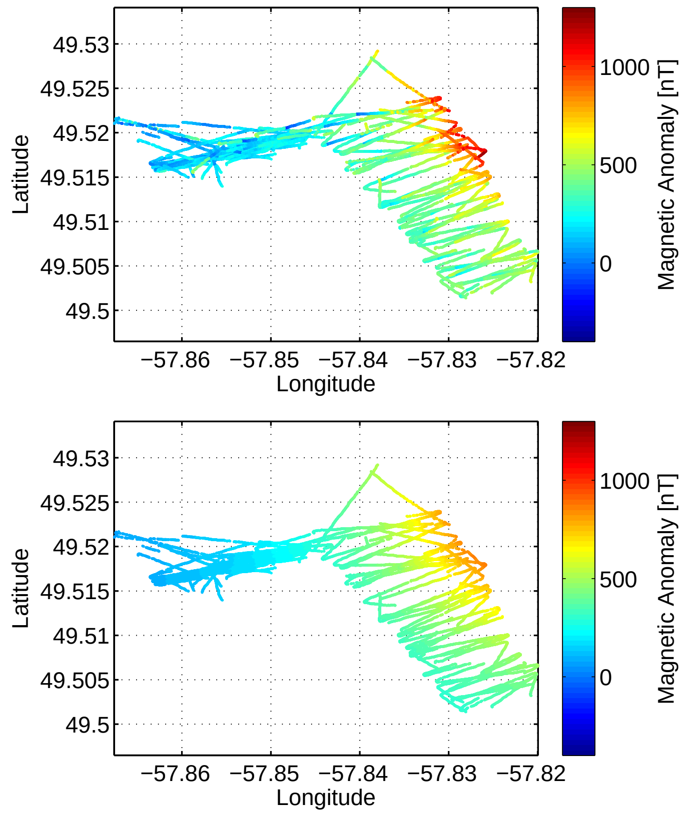

Fig. 6 Magnetic anomaly of the data collected during the Bonne Bay deployment in December 2013 calibrated using the parameterized geometric method (top) compared with the interpolated magnetic anomaly data from the aeromagnetic grids (bottom)

to the high levels of distortions which must be calibrated out of the magnetic measurements.

For rigid platforms with fixed components and low levels of electrical noise a geometric calibration method may be used. In this nominal geometric calibration method the raw measurements are assumed to lie on the surface of an ellipsoid. The ellipsoid's offset, radii and rotations of the major and minor axis form a set of calibration coefficients which may be used to correct the measurements in the sensor frame. For platforms with moving masses a parameterized geometric calibration method has been proposed. In this method a third order polynomial is estimated using gradient descent methods where the initial conditions are formed from the nominal geometric method parameters.

The parameterized calibration method is evaluated using an autonomous underwater glider equipped with a precision low power fluxgate magnetometer. During field trials of the system, which took place in December 2013 in the East Arm of

Bonne Bay, Newfoundland, calibration runs were performed upon deployment and before recovery. For each calibration run the underwater glider performed a series of descending and ascending spirals such that the mass shifting mechanism and ballast system were each at multiple steady state locations. Between these sets of calibration runs, the underwater glider ran its mission, cris-crossing up and down the East Arm. To obtain the parameterized calibration coefficients the complete set of calibration measurements from each run was used to extract the nominal ellipsoid coefficients. These nominal coefficients were then used as the initial conditions for the gradient descent solver which computed the third order polynomial coefficients which define each ellipsoid coefficient for the given mass shifter and ballast mechanism location.

The parameterized calibration method resulted in an RMS error between the calibration measurements and the local total field of 29 nT and 17 nT for the first and second set of calibration runs. During the survey portion of the field trials the first and second set of parameterized calibration coefficients resulted in a RMS error between the calibrated measurements and the local total field from the a-priori grid of 124 nT and 69 nT respectively.

Magnetic measurements performed in this manner are suited to the online calibration of magnetic data. This online correction is the ultimate goal of this work towards allowing the augmentation of terrain relative navigation methods with magnetic anomaly measurements.

Acknowledgments

This work was supported by the Natural Sciences and Engineering Research Council (NSERC) through the NSERC Canadian Field Robotics Network (NCFRN), the Research Development Corporation, the Marine Institute and Memorial University of Newfoundland.

References

1. Bartington Instruments: Mag648 and Mag649 Low Power Three-Axis Magnetic Field Sensors, Bartington Instruments, DS2298/9, retreived July 2011. (2011)
2. Bronner, A., Munschy, M., Sauter, D., Carlut, J., Searle, R., Maineult, A.: Deep-tow 3C magnetic measurement: Solutions for calibration and interpretation. Geophysics **78**(3), J15–J23 (2013)
3. Honarvar, P., Nolan, L., Crisby-Whittle, L., Morgan, K.: The geoscience atlas. Report 13-1, Newfoundland and Labrador Department of Natural Resources (2013). Geological Survey
4. International Association of Geomagnetism and Aeronomy, Working Group V-MOD. Participating members, Finlay, C.C., Maus, S., Beggan, C.D., Bondar, T.N., Chambodut, A., Chernova, T.A., Chulliat, A., Golovkov, V.P., Hamilton, B., Hamoudi, M., Holme, R., Hulot, G., Kuang, W., Langlais, B., Lesur, V., Lowes, F.J., Lhr, H., Macmillan, S., Mandea, M., McLean, S., Manoj, C., Menvielle, M., Michaelis, I., Olsen, N., Rauberg, J., Rother, M., Sabaka, T.J., Tangborn, A., Tffner-Clausen, L., Thbault, E., Thomson, A.W.P., Wardinski,

I., Wei, Z., Zvereva, T.I.: International geomagnetic reference field: the eleventh generation. Geophysical Journal International **183**(3), 1216–1230 (2010)
5. Isezaki, N.: A new shipboard three-component magnetometer. Geophysics **51**(10), 1992–1998 (1986)
6. Kato, N., Shigetomi, T.: Underwater navigation for long-range autonomous underwater vehicles using geomagnetic and bathymetric information. Advanced Robotics **23**(7-8), 787–803 (2009)
7. Kinsey, J.C., Eustice, R.M., Whitcomb, L.L.: A survey of underwater vehicle navigation: Recent advances and new challenges. In: IFAC Conference of Manoeuvering and Control of Marine Craft. Lisbon, Portugal (2006). Invited paper
8. Korenaga, J.: Comprehensive analysis of marine magnetic vector anomalies. Journal of Geophysical Research: Solid Earth (1978–2012) **100**(B1), 365–378 (1995)
9. McPhail, S., Stevenson, P., Pebody, M., Furlong, M.: The NOCS long range AUV project. In: National Marine Facilities Department Seminar Series (2008)
10. M.E.Furlong, McPhail, S., Stevenson, P.: A concept design for an ultra-long-range survey class AUV. In: Proc. of IEEE Oceans - Europe, pp. 1 –6 (2007)
11. Primdahl, F.: The fluxgate magnetometer. Journal of Physics E: Scientific Instruments **12**(4), 241 (1979)
12. Prouty, M., Johnson, R.: Small, low power, high performance magnetometers. In: EGM 2010 International Workshop (2010)
13. Renaudin, V., Afzal, M.H., Lachapelle, G.: Complete triaxis magnetometer calibration in the magnetic domain. Journal of sensors **2010** (2010)
14. Rudnick, D., Davis, R., Eriksen, C., Fratantoni, D., Perry, M.: Underwater gliders for ocean research. Marine Technology Society Journal **38**, 73–84 (2004)
15. Shah, V., Knappe, S., Schwindt, P.D.D., Kitching, J.: Sub-picotesla atomic magnetometry with a microfabricated vapour cell. Nature Photonics **1**, 649–652 (2007)
16. Teixeira, F.C., Pascoal, A.M.: Geophysical navigation of autonomous underwater vehicles using geomagnetic information. In: 2nd IFAC Workshop Navigation, Guidance and Control of Underwater Vehicles (2008)
17. Vasconcelos, J., Elkaim, G., Silvestre, C., Oliveira, P., Cardeira, B.: Geometric approach to strapdown magnetometer calibration in sensor frame. Aerospace and Electronic Systems, IEEE Transactions on **47**(2), 1293 –1306 (2011)